European Polymer Journal 148 (2021) 110362

Contents lists available at ScienceDirect

European Polymer Journal

journal homepage: www.elsevier.com/locate/europolj

The effect of matrix on shape properties of aromatic disulfide based epoxy vitrimers

Itxaso Azcune [a,*], Arrate Huegun [a], Alaitz Ruiz de Luzuriaga [a], Eduardo Saiz [b], Alaitz Rekondo [a]

[a] CIDETEC, Basque Research and Technology Alliance (BRTA), Paseo Miramón, 196, 20014 Donostia-San Sebastián, Spain
[b] Department of Materials, Centre for Advanced Structural Ceramics, Imperial College London, London SW72AZ, UK

ARTICLE INFO

Keywords:
Vitrimer
Aromatic disulfide
Epoxy network
Shape memory
Reprocessability

ABSTRACT

Aromatic disulfide based vitrimers show elasticity driven shape-memory and plastic reprocessability *via* associative rearrangement of dynamic covalent crosslinks. Those processess represent the two sides of a coin: the storage and relaxation of the strain energy caused by a deformation load. The key temperatures that trigger the underlying mechanisms, i.e. phase transition and disulfide exchange reaction, are extremely sensitive to the molecular structure of the polymer and under certain condition overlap. To gain insight on the relationship between the structure, dynamic and shape-changing properties, five aromatic disulfide-based epoxy networks with a range of T_g values (32–142 °C), molecular structure and crosslink densities (2252–462 mol m^{-3}) were synthesized. The epoxy matrices were formulated combining different ratios of rigid bisphenol A diglycidyl ether (DGEBA) and flexible poly(propylene glycol) diglycidic ether (DGEPPG) epoxy monomers crosslinked by 4-aminophenyldisulfide hardener.

1. Introduction

The combination of elasticity driven shape-memory and plastic reprocessability *via* associative rearrangement of dynamic covalent crosslinks has derived into fascinating shape-changing materials [1].

Shape memory polymers (SMPs) are known since the 1950s and they have been applied in a variety of areas, from self-deployable aerospace structures to biomedical applications [2,3]. From the structural perspective, SMPs are chemically or physically crosslinked materials that present a thermal transition (T_{trans}) that plays as a switch between the different shapes, i.e. the permanent and temporary shapes. In case of amorphous polymers this occurs at glass transition temperature (T_g) when the material becomes soft upon heating and brittle upon cooling. The programming starts by heating and applying a deformation on the permanent shape, followed by a rapid cooling to lock the new temporary shape. The deformation energy is stored in the new strained chain conformation until the increase of temperature permits molecular mobility and triggers the recovery of the permanent shape. The spontaneous shape recovery is attributed to the tendency of the network to increase its entropy until the crosslinking sites return to their original spatial positions, and it is driven and limited by the elastic properties of the material.

One feature of traditional crosslinked polymers or thermosets is that once the polymerization reaction takes place, the material cannot be reshaped or reprocessed above the elastic limits without irreversible structural damage. However, the incorporation of dynamic chemistry in polymer networks opened new possibilities [4–7]. There are materials, known as vitrimers, crosslinked with exchangeable bonds that can rearrange thermally (or under another stimulus) via a associative-mechanism and maintain network integrity [8–10]. This malleability of the network provides the crosslinked material with new functionalities such as, reprocessing, repairing and recycling, and allows setting new relaxed permanent shapes. There are two transition temperatures that drastically affect the viscoelastic properties of vitrimers: the freezing topology temperature (T_v) and the glass transition temperature (T_g). T_v represents the temperature below which the chemical exchange is expected to be negligible within the network. It is theoretically defined as the temperature at which the viscosity is 10^{12} Pa s [11–14]. Tg is the temperature at which the materials turns from a glassy to a rubbery state. Only when those two temperatures are exceeded, time-dependent relaxation yields a new relaxed shape.

SM vitrimers represent a paradigm of smart and modulable shape-changing materials. Those materials can be programmed to change temporary shapes under external stimuli and be recycled into new

* Corresponding author.
E-mail address: iazcune@cidetec.es (I. Azcune).

https://doi.org/10.1016/j.eurpolymj.2021.110362
Received 10 November 2020; Received in revised form 10 February 2021; Accepted 16 February 2021
Available online 1 March 2021

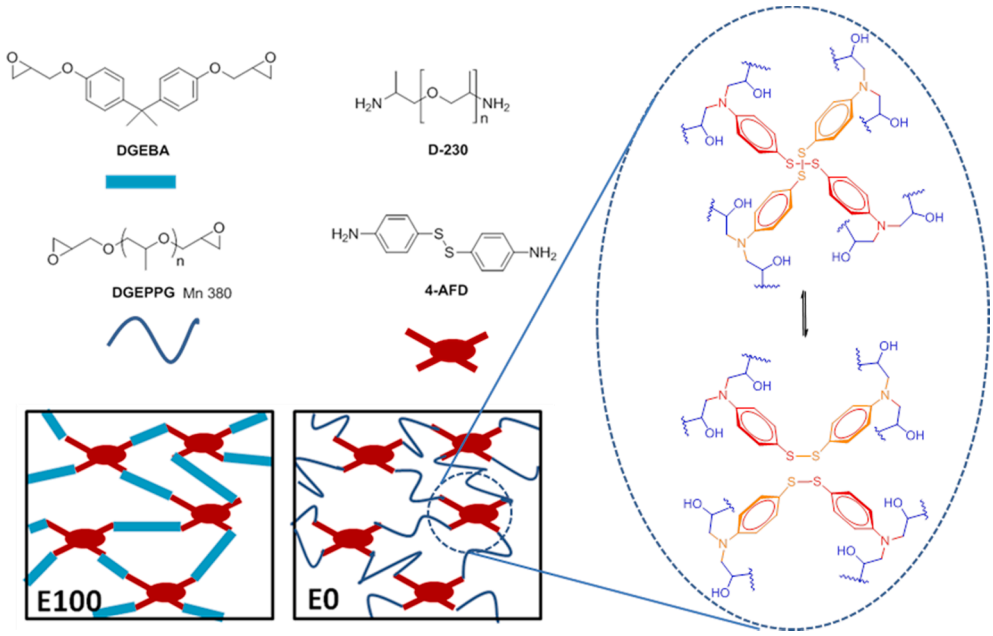

Fig. 1. Chemical structure of diepoxy and diamine network components and schematic representation of E100 and E0 networks with exchangeable aromatic disulfide crosslinks.

relaxed shapes albeit their crosslinked molecular structure.The majority of reported SM epoxy vitrimers present T_gs, in the range of 70–100 °C and rely on catalyzed transesterification for their plasticity which requires high temperatures (in the range of 160–200 °C) to be efficiently reprocessed [1,15–19]. Those SM epoxy vitrimers present a remarkable thermal gap between the shape-memory programming temperature and network rearrangement temperature ($T_v \gg T_g$), and thus, SM can be programed without endangering the storage of the strain energy in the temporary shape by the stress relaxation *via* crosslink exchange. Interestingly, SM vitrimers provide the opportunity to modulate the extent of shape recoveries by selecting the appropriate conditions to induce stress relaxation when setting the temporary shape. That was first shown in strain recovery tests carried out under irradiation using networks with photoinduced plasticity [20]. This is especially critical for SM vitrimers whose T_v is lower than T_g values. In those cases, the crosslink exchange is only hindered by insufficient molecular mobility (high viscosity), and the time and temperature dependent relaxation begin as soon as the system reaches T_g. Aroamtic disulfide-based vitrimers fall in that category. Aromatic disulfide exchange can take place even at ambient temperature without a need of a catalyst as shown by autonomous room temperature self-healing of aromatic disulfide based poly(urea-urethane) elastomers [21]. The pioneering work carried out on the reprocessing of aromatic disulfide based epoxy vitrimer (T_g 130 °C and T_v 75 °C), showed that stress relaxation occurred close to Tg (130 °C, 3 h), although higher temperatures (200 °C, 20 s) were required for rapid reprocessing [22]. Later, the concept of tunable shape recovery in disulfide base vitrimers was qualitatively demostrated in various shape memory tests by comparing two analogue isosorbide-based epoxies. [23]. Recently, Yang et al. took advantage of the shape-changing properties of aromatic disulfide based network to prepare composites with multi-shape memory by chemically welding materials with different switching temperatures [24]. Research on aromatic disulfide vitrimers is active, and a variety of papers dealing with different aspects, such as the synthesis of vitrimers from new epoxy monomers and hardeners [25–27] or the effect of the concentration of exchangeable group concentration on dynamic properties [28], have been reported recently.

Importantly, it has been claimed that the reactivity and the dynamic properties of vitrimers is likely to be influenced by the composition and molecular structure of the polymer matrix [14,29]. Here, we present a systematic characterization of aromatic disulfide-based epoxy vitrimers in order to correlate their viscoelastic, thermo-mechanical and dynamic properties, with the crosslinking density and polarity of the matrix (Fig. 1). With that objective in mind, a set of 5 aromatic disulfide-based epoxy vitrimers with a range of T_g values (142–32 °C), molecular structure and crosslink densities (2252–462 mol m^{-3}) were synthesized. Those epoxy matrices were formulated combining different ratios of rigid bisphenol A diglycidyl ether (DGEBA) and flexible poly(propylene glycol) diglycidic ether (DGEPPG) epoxy monomers crosslinked by 4-aminophenyldisulfide (AFD). The structure–property relationship of the material was assessed by TGA, DSC, DMA and swelling tests. Additionally, the tunability of shape memory properties where investigated by visual and quantitative thermomechanical tests. To that end, stress-relaxation was investigated in order to quantify the dissipation of the strain-energy at relevant temperatures, and the impact of time and temperature on the shape memory properties, i.e. fixity rate (R_f) and recovery rate (R_r), were measured by thermomechanical cycles. Besides, disulfide-free but structurally analogue epoxy thermoset was synthesized starting from DGEBA and poly(propylene glycol) bis(2-aminopropyl ether) (D-230) for comparison purposes.

Table 1
Formulation of epoxy networks.

Ref.	DGEBA/DGEPPG/AFD (mol ratio)	DGEBA	DGEPPG	AFD	D-230
R100	–	10.00 g	–	–	3.72 g
E100	1.0/0/0.55	10.00 g	–	4.00 g	
E75	0.75/0.25/0.55	7.29 g	2.71 g	3.90 g	–
E50	0.50/0.50/0.55	4.72 g	5.28 g	3.79 g	–
E25	0.25/0.75/0.55	2.30 g	7.70 g	3.69 g	–
E0	0/1.0/0.55	–	10.00 g	3.60 g	–

2. Experimental

2.1. Materials

DGEBA-based epoxy resin (Araldite LY1564, epoxide equivalent weight 161–173 g eq^{-1}) was purchased from Huntsman Advanced

Materials. Poly(propylene glycol) diglycidyl ether (DGEPPG, Mn = 380, epoxide equivalent weight 190 g eq^{-1}) was purchased from Sigma Aldrich. 4-Aminophenyldisulfide (AFD) was purchased from Molekula. Poly(propylene glycol) bis(2-aminopropyl ether) (D-230) was purchased from Sigma Aldrich. All chemicals were used as received.

2.2. Synthetic procedures

Corresponding amounts of DGEBA, DGEPPG and AFD were mixed at 80 °C and degassed under vacuum (Table 1). The resulting viscous liquid was poured into the interlayer space (2 mm) between teflon-coated two glass sheets and cured at 120 °C for 2.5 h and post-cured at 150 °C for 2 h. The reference R100 was synthesized starting from DGEBA and D-230 and cured at 100 °C for 1.5 h and post-cured at 130 °C for 1 h. The specimens were cut to the dimensions required for the characterization tests using a knife or a milling machine.

2.3. Characterization techniques

Fourier transformed infrared (FTIR) spectra were recorded on a JASCO-4100 spectrometer with a diamond ATR probe.

The thermogravimetric analysis (TGA) was performed on a TA Instruments Q500 equipment under air atmosphere at a heating rate of 10 °C min^{-1} from 25 °C to 800 °C. Isothermal tests were carried out at 200 °C under air atmosphere.

Differential Scanning Calorimetry (DSC) measurements were performed using a TA Instruments Discovery DSC 25 Auto over a temperature range from 25 °C to 220 °C under nitrogen atmosphere. Glass transition temperatures (T_g) were obtained as the inflection point of the second heat flow step recorded at a scan rate of 20 °C min^{-1}.

Macroscopic scale reprocessing experiments were carried out using a VOGT hot press LaboPress 200 T. Small sample pieces were compressed into thin sheets at selected temperature (140 °C −190 °C) under 100 bar for 10 min. The materials were allowed to reach room temperature in open mold.

Stress-relaxation experiments were carried out in a TA instrument AR2000ex rheometer. Circular samples of 8 mm diameter were used for the experiments. Samples were allowed one minute to reach the thermal equilibrium at testing temperature. The specimens were stretched by 1% and the deformation was maintained during the test. The decrease of stress over time was recorded and the stress relaxation modulus was calculated.

Thermo mechanical and quantitative shape memory experiments were performed using TA Instruments DMA Q800 equipment equipped with a gas cooling accessory (GCA). For the thermo mechanical experiments the mode of deformation applied was the single cantilever beam, and the dimensions of samples were 12.5 × 2 × 17.5 mm^3. The temperature range varied from −40 °C to 80 °C for sample E0; from 25 °C to 150 °C for samples E50 and E25; and from 25 °C to 180 °C for samples E75 and E100. The temperature dependent behavior was studied by monitoring changes in force and phase angle, keeping the strain amplitude at 0.01% (within linear viscoelastic region, ESI Fig. 6) and frecuency (1 Hz) constant at a 2 °C min^{-1} heating rate. The quantitative shape memory behavior of the materials was evaluated using a tensile film fixture and the controlled force mode. The sample was first heated to T_{trans} at 10 °C min^{-1} heating rate; then the sample was stretched 1.5 N min^{-1} to 1.5 N. The sample was hold for a controlled exposure time and cooled to 25 °C at 15 °C min^{-1} heating rate maintaining the load (registered strain defined as ε_{load}). After 10 min, the sample was unloaded 1.5 N min^{-1} to 0.001 N, the length of the sample in the temporary shape was obtained (registered strain defined as ε_{unload}). The recovery process was then triggered by heating the sample back to T_{trans} with a heating rate of 10 °C min^{-1} (registered strain defined as ε_{rec}). Each experiment was repeated twice where 2 and 3 cycles were recorded. The shape fixity ratio (R_f) and shape recovery ratio (R_r) were determined using the Eqs. (1) and (2):

$$R_f = \varepsilon_{unload}/\varepsilon_{load} \times 100\% \quad (1)$$

$$R_r = (\varepsilon_{unload} - \varepsilon_{rec})/\varepsilon_{unload} \times 100\% \quad (2)$$

In order to perform visual shape memory test, specimens with a permanent straight bar shape were deformed to a temporary U shape in an oil bath at T_g, holded for a controlled exposure time, and then, cooled in a water bath at ambient temperature to fix the temporary shape. The specimen with the temporary fixed shape was then placed back in hot oil to trigger the shape recovery and recovery angle. Deviation from initial straight shape (0°) was measured.

Water absorption test were also performed. First, the specimens (15 mm × 45 mm × (1–2) mm) were dried in an oven at 150 °C until constant weight was registered. Epoxy specimens were inmersed in a water bath at 20 °C and periodically samples were weighted during 11 days. Since the samples did not reach the equilibrium, the temperature was raised to 80 °C and the water absortion was registered for 50 days. After this time, the samples were dried and T_g was measured and compared to pristine T_g to evaluate the degradation of the network.

Table 2
Thermal decomposition and glass transition temperatures.

Ref.	T_{onset}^{TGA} (°C)	T_g^{DSC} (°C)	T_g^{DMA} (°C)
R100	319	70	77
E100	290	140	142
E75	271	105	114
E50	263	75	88
E25	258	56	66
E0	200	39	44

3. Results and discussion

3.1. Synthesis of aromatic disulfide based epoxy vitrimers

Five dynamic networks with different molar percentages of diepoxides (DGEBA/DGEPPG) were synthesized: E100 (100/0), E75 (75/25), E50 (50/50), E25 (25/75) and E0 (0/100). The chemical structures of the reactants and the formulation of each system are shown in Fig. 1 and Table 1, respectively. In all the formulations 1.1 equivalent of AFD was used per 1.0 epoxy equivalent. Additionally, R100 thermoset was synthesized for comparative purposes starting from DGEBA and D-230. The epoxy networks were prepared by mixing the epoxy monomers and the hardener followed by a curing cycle at high temperatures. The complete curing of the networks was confirmed by the lack of residual exothermic peak at the first scan of the DSC thermogram. Additionally, the complete curing was assessed by FTIR (ESI Fig. 1) following the criteria of the disappearance of the epoxy functional group at 915 cm^{-1} (C—O stretching) and 3056 cm^{-1} (C—H stretching), as well as the increase of the peak at 3370 cm^{-1} attributed to the new hydroxyl group generated upon the oxirane opening.

3.2. Thermal and thermo-mechanical characterization

Thermal properties of the epoxy networks depend on compositional and structural factors such as stiffness of polymer segments, interchain cohesive forces and crosslinking. The flexibility and length of the molecular segments differ considerably within the E series, and thus, distinct thermal and mechanical properties are expected. TGA, DSC and DMA techniques were used to measure thermal stability and T_g temperatures (Table 2).

All DSC thermograms displayed a single thermal transition in the experimental temperature range which was attributed to the T_g (Fig. 2a). The incorporation of a flexible monomer lowered T_g values [30]. Such thermogram profiles also proved that the networks had an homogeneous phase structure. The T_g was also determined from the

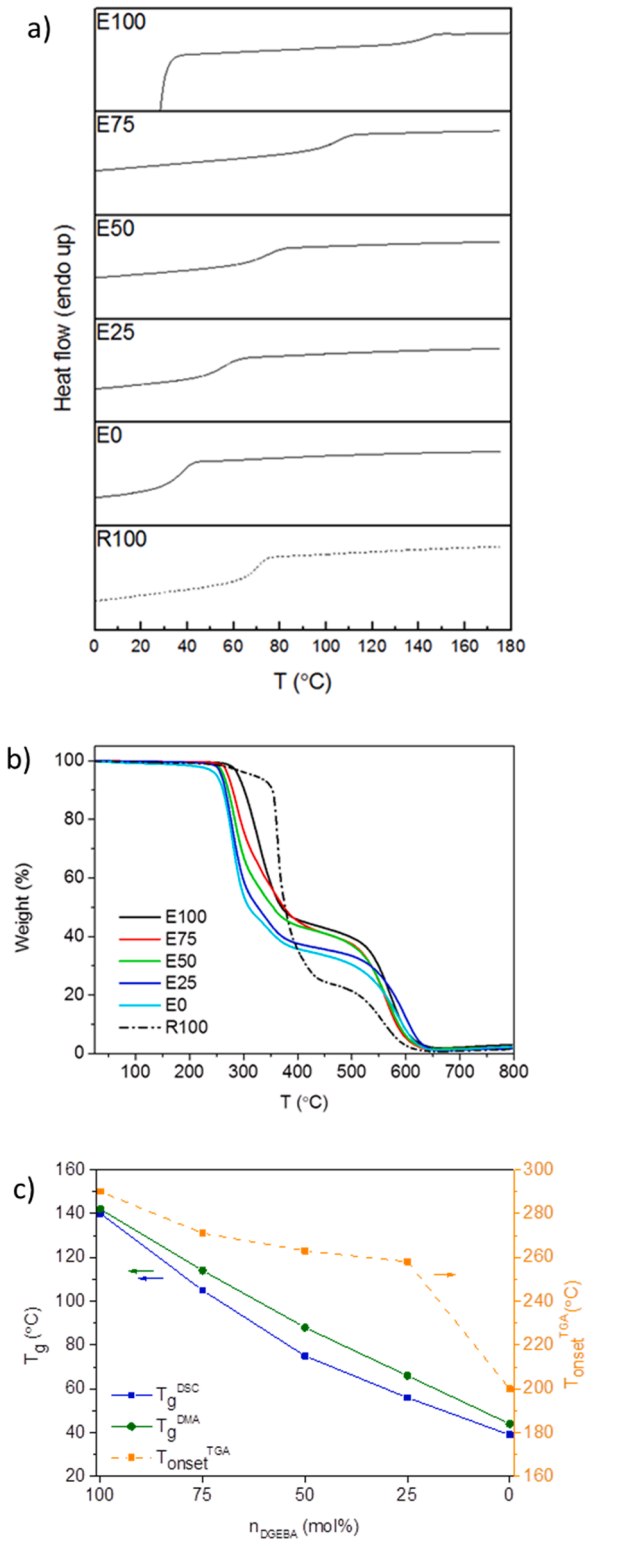

Fig. 2. Thermal characterization of networks: (a) DSC thermograms. (b) TGA thermograms in air. (c) Graphical representation of T_gs measured by DSC and DMA and T_{onset}^{TGA} measured by TGA of E series networks.

peak of tan δ recorded in the temperature ramp DMA tests (Fig. 3a). There is almost a linear relationship between the ratio of epoxy monomers and their T_g (Fig. 2c). Thus, any network with the desired T_g value (T_g^{DSC} between 142 °C and 39 °C) could be formulated. In practice, in order to employ ambient temperature as shape fixing temperature and avoid undesired flow and stress relaxation, materials should have

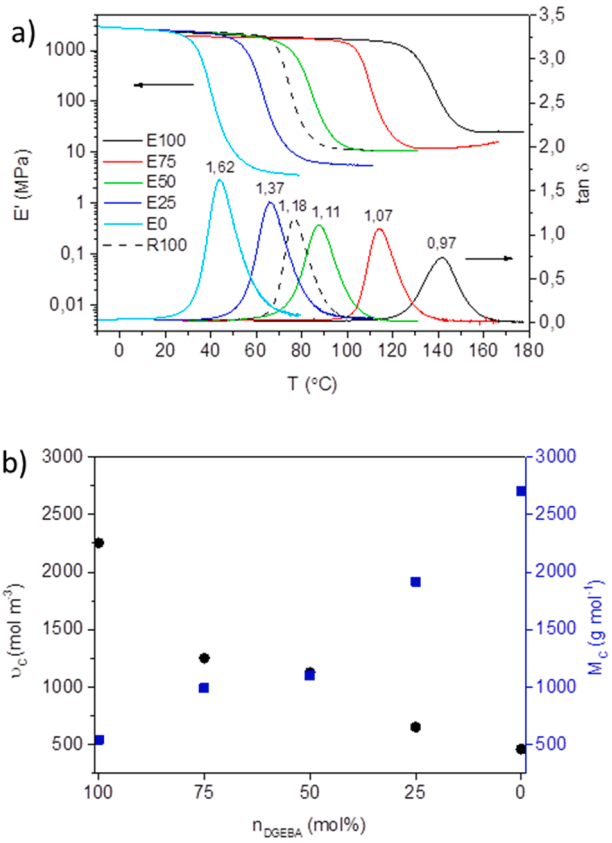

Fig. 3. (a) Temperature dependence of storage modulus (E') and tan δ of the epoxy networks. (b) Calculated crosslink density (ν_C) and molecular weight between crosslinks (Mc) of E series applying rubber elasticity theory.

sufficiently high T_g.

The thermal stability of the networks in air was evaluated by thermogravimetric analysis (Fig. 2b). Two observations were evident: (i) all epoxy networks decomposed in two apparent steps, and (ii) the onset temperature, T_{onset}^{TGA} (i.e. the temperature of 5 wt% loss of material), was shifted to lower temperatures with increasing percentage of DGEPPG in the formulation. The registered T_{onset}^{TGA} values differed quantitatively from 290 °C of E100 to 200 °C of E0 (Table 2 and Fig. 2c). This is explained because rigid aromatic segments of DGEBA provide better thermal stability compared to flexible polyether chains [31]. Thus networks of E series that contain more DGEBA are thermally more stable, and that the lack of it lowers considerably the T_{onset}^{TGA}. Additional isothermal tests were carried out with E75, E50 and E25 samples to simulate extreme reprocessing (permanent shape modification) conditions (ESI Fig. 2). At 200 °C for 30 min under air, samples showed no-significant weight loss (0.66–1.25 wt%) and no structural degradation was evidenced since T_g values measured after the tests were in accordance with T_gs of pristine materials. R100 sample showed the highest T_{onset}^{TGA} among all samples. This is attributed to the lack of the weak disulfide moieties which lower the overall thermal stability of the E series epoxy matrices.

The temperature ramp DMA test provides information about the relative contribution of viscous and elastic properties of the materials in the analyzed temperature range, i.e. storage modulus (E'), loss modulus (E'') and tan δ which is the ratio of E'' to E'. The height of tan δ indicates the energy dissipation potential of the material; and in general, the higher the tan δ value, the better are the damping properties. In the E series the maximun tan δ values range between 0.97 and 1.62, corresponding to lower and higher DGEPPG flexible segment concentration in the network (Fig. 3a).

The weigth percentage of the dynamic hardener in the networks fall in the range of 29–27 wt% corresponding to E100 and E0, respectively.

Table 3
Density, ν_C and M_C of the networks applying rubber elasticity theory.

Ref.	Tan δ max.	E' (10^6 Pa) at T_g^{DMA} + 30 K	D (10^6 gm^{-3})	ν_C (molm^{-3})	M_C (gmol^{-1})	Swelling[1] (%)	Water uptake[2] (%)	
							20 °C	80 °C
R100	1.18	11	1.15	1161	990	–[3]	–[3]	–[3]
E100	0.97	25	1.22	2252	542	4.2	0.85	2.9
E75	1.08	13	1.24	1250	992	17.9	0.66	3.8
E50	1.11	11	1.24	1128	1099	30.8	0.74	10.4
E25	1.37	6	1.25	652	1917	33.3	1.81	35.1
E0	1.62	4	1.25	462	2706	40.3	2.92	53.7

[1] Weight gain in acetone in equilibrium.
[2] Equilibiurm not reached after 11 days at 20 °C and after 50 days at 80 °C.
[3] Not measured.

This is because diepoxy monomers have similar epoxy equivalent weight (EEW), 170 g eq^{-1} DGEBA and 190 g eq^{-1} DGEPPG, and all were formulated with 1.1 equivalent of AFD. Additionally, the densities of the networks are between 1.22 g ml^{-1} and 1.25 g ml^{-1}. Thus, it can be concluded that the disulfide juncture concentration is similar in the whole E series. However, the two diepoxy monomers differ in the chain length and flexibility which certainly leads to completely different network structures. DGEBA has a rigid aromatic backbone, whereas DGEPPG provides a flexible polyether segment. The crosslink density (ν_C) provides an idea of the network structure which is defined as the number of elastically effective network chains per unit volume of the sample. For an amorphous thermoset, ν_C can be experimentally obtained applying the rubber elasticity theory above its T_g (Eq. (3)).

$$\nu_C = E'/3{\cdot}A{\cdot}R\ T \quad (3)$$

where E′ is measured in the rubbery plateau (30 °C above T_g^{DMA}); A is the front factor often assumed to be unity; R is the gas constant (8.314 J mol^{-1} K^{-1}) and T is equal to T_g^{DMA} + 30 K. The ν_C can be also described in terms of average molecular weight between crosslinks (M_C) (Eq. (4)).

$$M_C = d/\nu_C \quad (4)$$

where d is the cured resin density.

The difference between the composition of R100 and E100 is the diamine hardener (D230 and AFD, respectively), since in both formulations the epoxy monomer is DGEBA. R100 contains the flexible and long D-230 whereas E100 contains the short aromatic AFD. The difference in crosslinking density, i.e. 100 showing higher crosslinking density than R100, is attributed to those structural differences. As expected, within the E series, replacing DGEBA by the flexible DGEPPG monomer (presenting same main chain that D-230) leads to substantial decrease of ν_C and associated increase of M_C (Table 3). The measured data shows that crosslinking density of R100 and E75/E50 are comparable and this is attributed to a similar balance of flexible and rigid segments.

These calculations are experimentally supported by the results of equilibrium swelling tests in an organic solvent since swelling is closely related to crosslinking density (Table 3). To do so samples were submerged in acetone and weight gain was monitored until equilibrium was reached. The solvent gain is in line with the capability of expansion of the network, the lower the crosslinking density, the higher the swelling capability.

Another important structural difference among the networks are their polarity and water absorption capability. Epoxy matrices easily absorb water when exposed to humid environments due to polar hydroxyl groups. The extent of water absorption is further enhanced by the polarity of the matrix and its swelling capability. In this series, both variables point in the same direction due to highly hydrophilic and flexible polyether DGEPPG segments. To assess this (ESI Fig. 3), specimens were immersed in water at ambient temperature (ca 20 °C), and the weight gain was monitored for eleven days. During this period of time samples did not reach equilibrium: the larger uptake was for E0 (2.92 wt%) followed by E25 (1.81 wt%); the rest of the samples showed smaller weight gain (0.66–0.86 wt%). Aiming at accelerating the absorption and highlight the structural differences, the temperature was raised up to 80 °C and the weight gain was monitored. Ater 50 days, only E100 (2.9 wt%) and E75 (3.8 wt%) reached the plateau; E50 (10.4 wt%), E25 (35.1 wt%) and E0 (53.7 wt%) showed an upward trend. After this time samples were dried and T_g^{DSC} of the materials were measured to assess any structural damage (i.e hydrothermal degradation) (ESI Fig. 4 and ESI Table 1). The T_gs measured by DSC were in line with starting values. The high water uptake of the samples evidenced their high susceptibility to plasticization under humidity conditions which has a dramatic effect on lowering T_g and affecting mechanical (lowering modulus) and shape memory properties.

3.3. Stress relaxation and creep tests

Vitrimers based on aromatic disulfide crosslinks undergo associative type exchange [32–33]. Applying pressure and temperatures above T_g and T_v, materials can be reprocessed into new shape albeit their

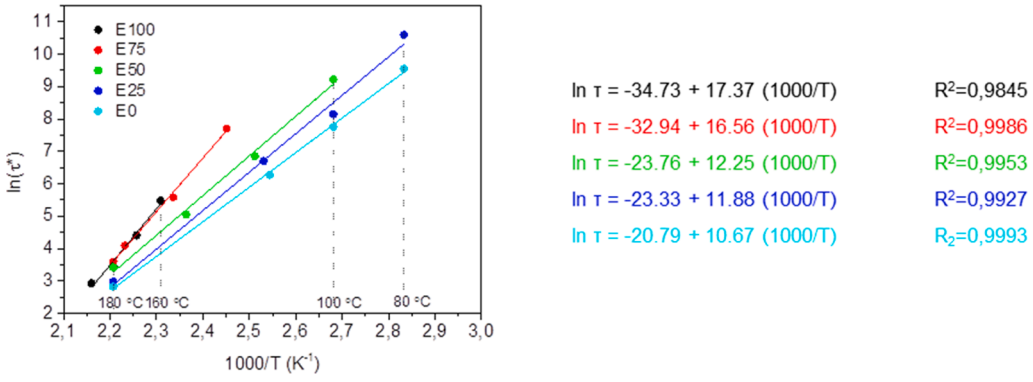

Fig. 4. Fitting of the relaxation times to the Arrhenius's equation.

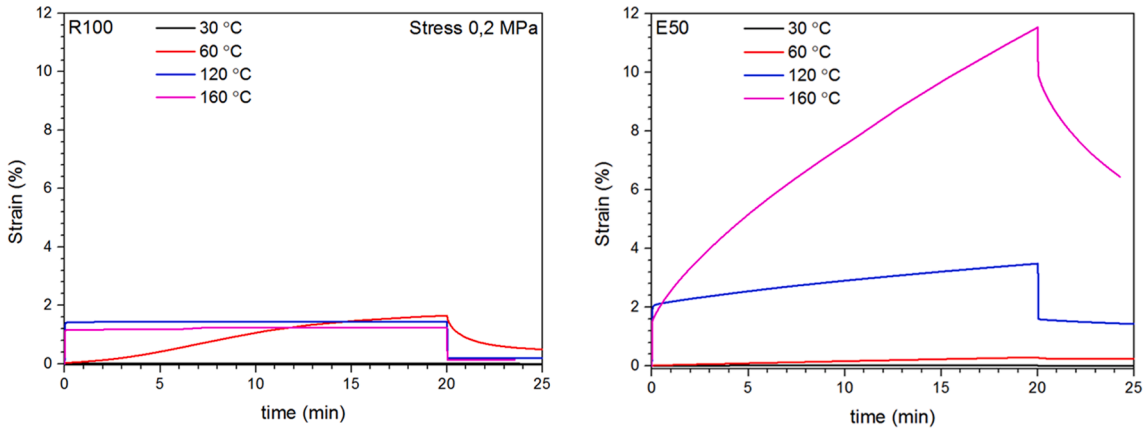

Fig. 5. Creep experiment of R100 (T_g^{DMA} = 77 °C) and E50 (T_g^{DMA} = 88 °C) at 30 °C, 60 °C, 120 °C and 160 °C.

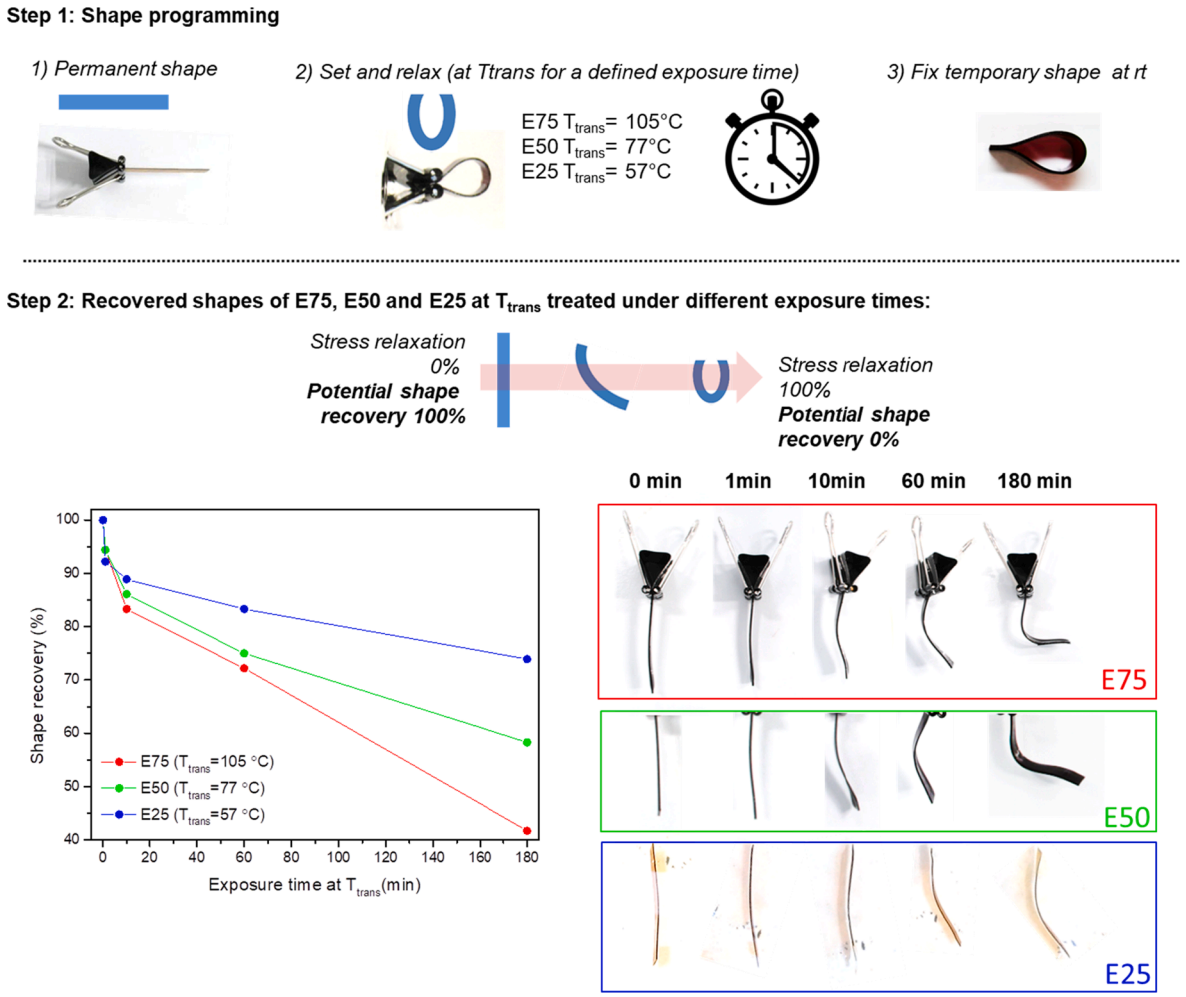

Fig. 6. Visual shape memory tests of E75, E50 and E25.

crosslink structure. Small pieces of cured dynamic epoxies were reprocessed into flat homogeneous thin sheets (ESI Fig. 5). For comparative purposes, the same compression was applied to R100 which showed no malleability and reprocessing capability, and showed multiple cracks.

Then, stress relaxation of the networks was investigated in the rheometer applying shear deformations and monitoring the stress (ESI Fig. 7). Relaxation time (τ*) was calculated following the Maxwell model which defines it as the time needed for the modulus to decrease to 37% of its initial value ($G/G_0 = 1/e$). τ* data as a function of the temperature follows the Arrhenius' law (Eq. (5)) and the corresponding plots are shown in Fig. 4.

$$\tau(T) = \tau_0 e^{\left(\frac{Ea}{RT}\right)} \tag{5}$$

where τ is the relaxation time at each temperature, Ea is the activation

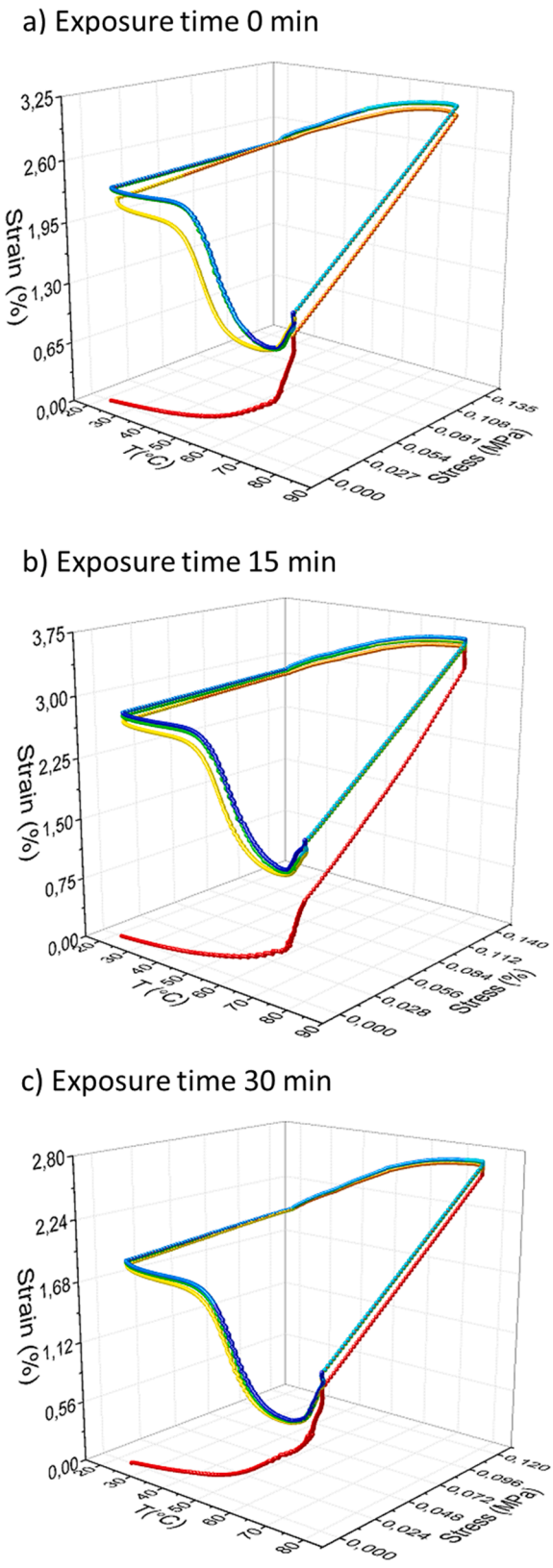

Fig. 7. Thermo mechanical cycles of E25 recorded setting different exposure times at T_{trans} (80 °C): (a) 0 min, (b) 15 min and (c) 30 min. Trajectory color coded for time: from red (t = 0 s) to dark blue.

Table 4
Ea, T_g^{DMA}, T_v and τ at various temperatureas (180 °C, T_g + 50 °C and T_v + 50 °C) of networks.

Ref	Ea (KJ mol^{-1})	τ* (s) at		T_g^{DMA} (°C)	T_v (°C)	ΔT (T_g^{DMA}-T_v)
		180 °C	T_g + 50 °C			
E100	144.4	37	14 (192 °C)	142	101	41
E75	137.6	37	312 (155 °C)	114	95	19
E50	101.8	26	953 (127 °C)	77	65	12
E25	98.7	18	1337 (116 °C)	66	53	13
E0	88.7	16	3698 (95 °C)	45	38	7

energy, R is the gas constant (8.314 J mol^{-1} K^{-1}) and T is the absolute temperature.

Two conclusions were drawn from Fig. 4: i) When comparing all the networks at a given temperature (T > T_g and T_v); the lower the T_g, the shorter the relaxation time of the network. This is attributed to the enhanced diffusion and exchange of reactive groups due to its lower crosslinking density and viscosity. ii) The higher the T_g of the network, the higher the Ea. This points out that the rate of exchange reaction has higher thermal dependency, i.e. a small thermal variation leads to bigger structural changes. In Table 4 Ea and interpolated τ values at various temperatures (180 °C and T_g^{DMA} + 50 °C) for each network are given. The Ea values could be grouped into two value sets: ca 140 KJ mol^{-1} (E100 and E75) and ca 100 KJ mol^{-1} (E50 and E25, slightly lower E0). The first set shows that small increase in temperature leads to a more pronounced reduction of τ compared to formulations from the second set. All plot lines converged at high temperature (e.g. the τ values of all networks are of the same order of magnitude at 180 °C), showing that the rate of exchange is not limited by viscosity anymore. The τ of each network at T_g + 50 °C differ substantially (3 orders of magnitude): for E100 it takes less than 20 s and for E0 1 h. This is explained by the distinct mobility and kinetic energy that the systems own in each case to promote the disulfide exchange and polymer chain movements. The fact that the dynamic properties of vitrimers are highly influenced that the exact composition and architecture of the matrix has been previously observed [9].

Additionaly, T_v was determined from Arrhenius' fitted line using a relaxation time calculated from the Maxwell equation (Table 4) [9]. The Maxwell relation η= Gτ*, correlates the viscosity (η=10^{12} Pa s) with relaxation time, G being the shear modulus. G was calculated from the tensile modulus (E') as measured by DMA from the relation G = E'/2(1 + v); with v = 0.5, the Poisson ratio usually used for rubbers (ESI Table 2). The calculated T_v temperatures were lower than the corresponding T_g, showing that as soon as intermolecular forces are overcome and molecular motion is gained, the exchange reaction takes place. The temperatures at which disulfide exchange reactions occur are extremely sensitive to the molecular structure and the T_g of the vitrimer. The thermal difference (T_g^{DMA}-T_v) was enhanced with increasing the T_g of the network.

Additional creep experiments at various temperatures were performed to compare the distinct behavior of a vitrimer and a thermoset without dyanamic bonds (Fig. 5). To do that E50 network was selected and compared to R100 in 30 min tests at four temperatures. Albeit not being structurally analogues, both networks are composed of aromatic and PPG segments, and present comparable T_g^{DMA} and v_C values.

At 30 °C neather of the networks presented a deformation under 0.2 MPa stress. R100 (T_g^{DMA} = 77 °C) strained around 1.75% at 60 °C, 120 °C and 160 °C to accommodate the applied stress. At temperatures well above the T_g the network was stretched instantly, and the the recovery of the elastic deformation also occurred right away. At 60 °C, both processes were progressive, most likely because the network was below T_g and the intermolecular interactions caused resistance. On the other

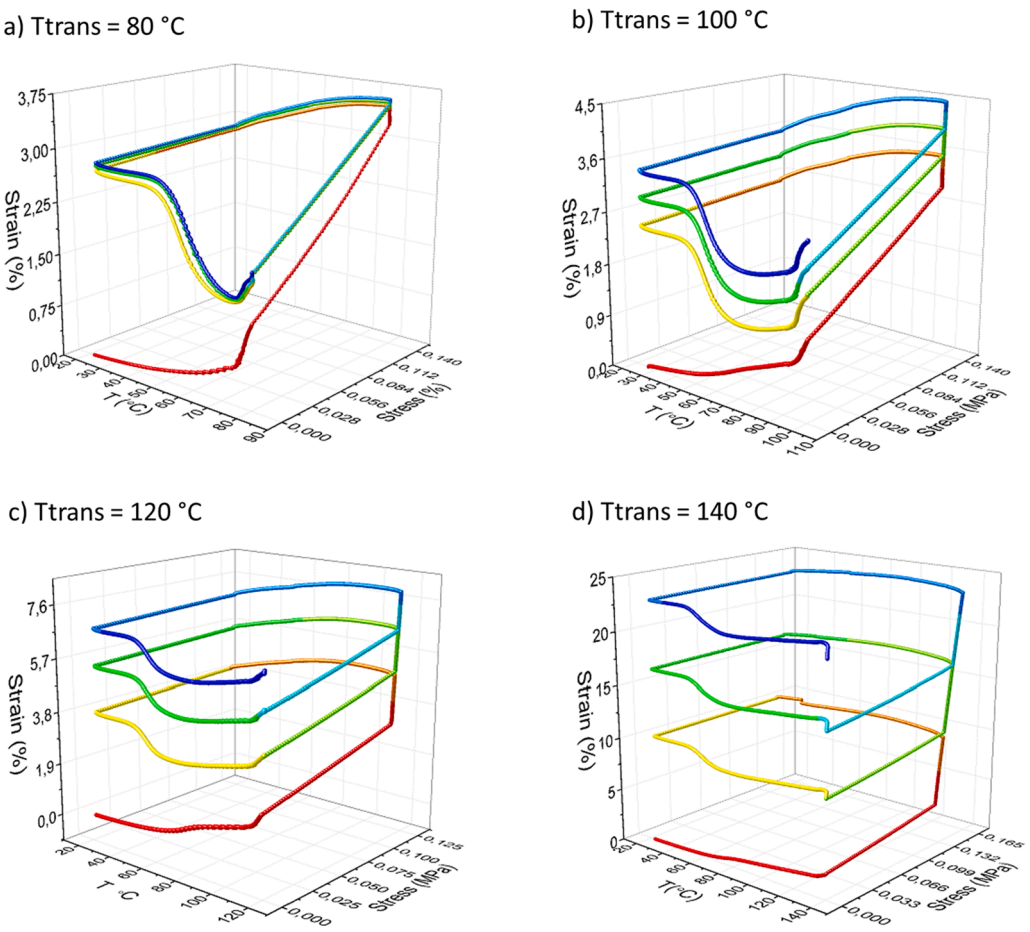

Fig. 8. Thermo mechanical cycles of E25 recorded setting 15 min exposure time at different T_{trans} temperatures: (a) 80 °C, (b) 100 °C, (c) 120 °C and (d) 140 °C. Trajectory color coded for time: from red (t = 0 s) to dark blue.

hand, E50 (T_g^{DMA} = 88 °C) presented negliable creep at 60 °C, but at 120 °C and 160 °C the strain increased rapidly with increasing temperature. This clearly indicates that the network can release the stress by continuous rearrangement of the network, overcoming the limits of the fixed network structure. Regarding the recovery, it was observed that the system first showed a partial instanteneous recovery followed a slower rate process. The deformation was not recovered quantitatively due the relaxation of the network.

3.4. Shape memory tests

The sharp drop in modulus and extended rubbery plateau observed in the temperature sweep in DMA are properties highly recommended for SMP materials. First, the shape memory properties were analyzed by visual experiment. The test was designed to compare shape recovery of E75, E50 and E25 networks when distinct exposure times (0 min, 1 min, 10 min, 1 h and 3 h) were set at the corresponding shape programming step (Fig. 6). The tests were performed at T_{trans} corresponding to T_g^{DSC} of each network (105 °C for E75, 77 °C for E50 and 57 °C for E25). Before the tests, one edge of each rectangular shape samples was covered with tape to avoid adhesion between network surfaces during the tests. For each experiment, a pristine rectangular shape specimen was heated to T_{trans} inside an oil bath, deformed into a closed U shape and holded with a binder clip for different time lapses. Then, the specimen was cooled down to ambient temperature in a water bath and the binder clip was removed. Finally, the samples were immersed in the oil bath at T_{trans} and the shape recovery was determined by measuring the deformation angle. We assumed that if there was no stress relaxation the sample would have the potential of recovering the initial flat rectangular shape (0° deformation angle, 100% recovery). In case complete stress relaxation occurred the specimen would fix the U shape (180° deformation, 0% recovery). At 0 min test all the networks recovered the initial permanent shape whereas at 3 h tests the deformation were pronounced. When it came to compare the three networks, the deformation associated to the stress relaxation was more evident for E75, followed by E50 and E25. The relaxation times associated to these temperatures were not experimentally measured and should have to be extrapolated from the stress relaxation test results (Fig. 4). In any case, the enhanced stress relaxation of E75 could be attributed to a faster exchange reaction activated by the higher temperature.

E25 network was selected to carry out quantitative thermo-mechanical cyclic tests in DMA in force controlled mode equipped with a GCA and tensile fixture to analyse the effect on Rf (%) and Rr (%) of two parameters, i.e. the exposure time at T_{trans} and the selected T_{trans}. Rf shows the ability of the material to fix the strain imposed on it after cooling and unloading the sample. It is also affected by the expansion coefficient of the resin which have not been determined in this work. On the other hand, Rr reflects the percentage of the initial strain that is recovered after the thermo-mechanical cycle. If the system recovers the initial strain in the "permanent shape" after re-heating the sample in the temporary shape, the Rr is 100%. The tests were carried out following the procedure described in the characterization techniques section and measured strain values are provided in ESI Table 3.

In order to study the effect of the exposure time at T_{trans} on the shape memory properties of E25 three experiments were carried out (Fig. 7). T_{trans} was set at 80 °C and different exposure times (0 min, 15 min and 30 min) were screened. It was observed that in the first thermo-mechanical cycle there was a major deformation that was not

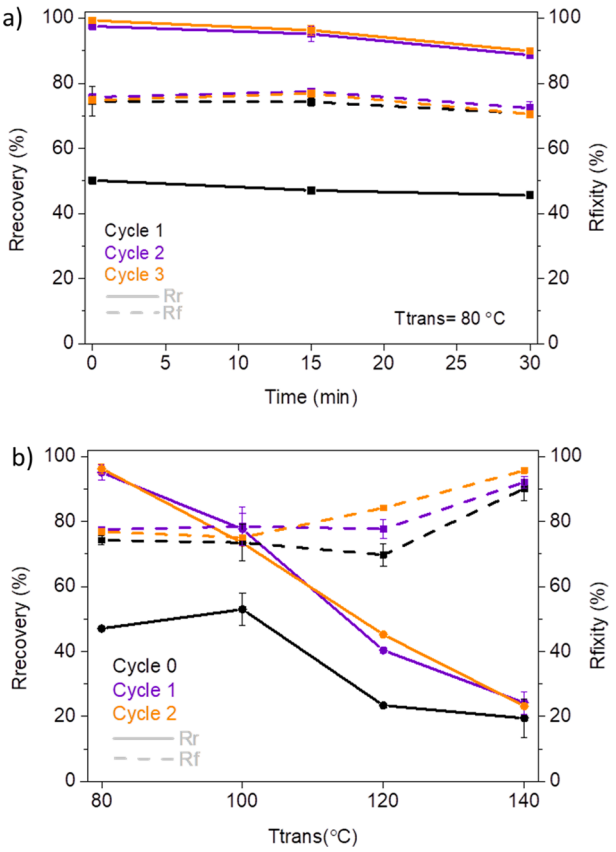

Fig. 9. Calculated Rr and Rf at different testing parameters: (a) Exposure time. (b) T_{trans}.

recoverable. This was attributed to the unrecoverable plastic deformation (e.g. uncoiling along stress axis) that is induced in cycle 1. In the subsequent cycles 2 and 3, the trajectories were overlapped. In Fig. 9a the calculated Rr and Rf are provided. The Rr of the fist cycle was around 50% in the tested temperatures, and in the subsequent cycles, the value showed a decreasing trend from almost 100% to 90%. Rf values obtained at different exposure times falled within 70–80% with no particular trend and could be likely be caused by thermal shrinkage of the matrices. It was concluded that at 80 °C the stress relaxation is slow and thus, exposure time has no significant effect on the shape recovery.

Then, the effect of temperature was investigated (Fig. 8). To that end, an exposure time of 15 min was set in isothermal conditions under load, and experiments were carried out at four different T_{trans} (80 °C, 100 °C, 120 °C and 140 °C). In Fig. 9b the calculated Rr and Rf are provided. It was evident that as temperature was increased the stress relaxation was enhanced and samples creeped, leading to extended strains after each cycle. Higher temperatures made the differences between cycles more pronounced. The Rr was reduced from 97% at 80 °C to 20% at 140 °C. The relaxation time of E25 at 140 °C was determined to be 3.8 min according to the corresponding Arrhenious plot, which explains the poor recovery. Regarding the Rf, the calculations pointed that the fixity was improved at higher temperature, but these numbers are just the consecuence of the lower influence of the thermal shrinkage on highly strained and yielded samples.

4. Conclusions

In this paper, the effect of matrix on the shape properties of aromatic disulfide based epoxy vitrimers was analyzed. The combination of flexible (DGEPPG) and rigid (DGEBA) epoxy monomers yielded matrices with varying molecular structure, polarity, crosslinking density and viscoelastic properties. The concentration of aromatic disulfide moieties within the vitrimer series was comparable. Therefore, their dynamic properties were exclusively attributed to the matrix structure, especially to their distinct Tg (32–142 °C) and viscosities. T_vs of all the networks were lower than the corresponding T_gs, indicating that, in all cases, the kinetics of molecular rearrangement is strongly hampered by frozen segmental motion at temperatures below T_g. The analysis of stress relaxation above T_g showed that at very high temperatures (180 °C), all the networks relaxed at a couple of tens of seconds. However, at lower temperatures, the rate of exchange is limited by the viscosity and diffusion of reactive groups within the matrix. The lower the T_g, the relaxation process becomes faster and less temperature dependent (lower activation energy, Ea). In any case, all the networks allowed setting new relaxed shapes under appropriate conditions. On the other hand, the high tunability of their shape memory properties was demonstrated. If the temporary shape was fixed instantaneously, the stress relaxation was found to be negligible. In that case, aromatic disulfide vitrimers showed quantitative shape recoveries (although the unrecoverable plastic deformation in the first cycle). However, by adjusting the exposure time and/or temperature during the shape programming step, it was possible to control the extent of the stress relaxation that prevails and limits the shape recovery. We consider that aromatic disulfide vitrimers can be regarded as versatile materials with highly tunable shape properties that can be exploited for multiple applications. The ease of synthesis of aromatic disulfide vitrimers (considering the wide pool of epoxy monomers available) allows designing materials accommodated to transition temperatures of interest.

CRediT authorship contribution statement

Itxaso Azcune: Conceptualization, Investigation, Writing - original draft preparation. **Arrate Huegun:** Investigation, Reviewing. **Alaitz Ruiz de Luzuriaga:** Investigation, Reviewing. **Eduardo Saiz:** Reviewing, Funding acquisition. **Alaitz Rekondo:** Conceptualization, Funding acquisition.

Declaration of Competing Interest

The authors declare that they have no known competing financial interests or personal relationships that could have appeared to influence the work reported in this paper.

Acknowledgements

This work has been financially supported by the Office of Naval Research (ONR) under award number N62909-18-1-2056.

Data availability statement

The raw/processed data required to reproduce these findings cannot be shared at this time due to technical or time limitations.

References

[1] Q. Zhao, W. Zou, Y. Luo, T. Xie, Shape memory polymer network with thermally distinct elasticity and plasticity, Sci. Adv. 2 (2016), 1 e1501297.
[2] P.T. Mather, X. Luo, I.A. Rousseau, Shape memory polymer research, Annu. Rev. Mater. Res. 39 (2009) 445–471.
[3] F. Pilate, A. Toncheva, P. Dubois, J.M. Raquez, Shape-memory polymers for multiple applications in the materials world, Eur. Polym. J. 80 (2016) 268–294.
[4] S.J. Rowan, S.J. Cantrill, G.R.L. Cousins, J.K.M. Sanders, J. Fraser Stoddart, Dynamic covalent chemistry, Angew. Chem. Int. Ed. 41 (2002) 898–952.
[5] J.M. Lehn, Dynamers: dynamic molecular and supramolecular polymers, Prog. Polym. Sci. 30 (2005) 814–831.
[6] T. Maeda, H. Otsuka, A. Takahara, Dynamic covalent polymers: reorganizable polymers with dynamic covalent bonds, Prog. Polym. Sci. 34 (2009) 581–604.

[7] C.J. Kloxin, T.F. Scott, B.J. Adzima, C.N. Bowman, Covalent adaptable networks (CANs): a unique paradigm in cross-linked polymers, Macromolecules 43 (2010) 2643–2653.
[8] D. Montarnal, M. Capelot, F. Tournilhac, L. Leibler, Silica-like malleable materials from permanent organic networks, Science 334 (2011) 965–968.
[9] W. Denissen, J.M. Winne, F.E. Du Prez, Vitrimers: permanent organic networks with glass-like fluidity, Chem. Sci. 7 (2015) 30–38.
[10] W. Zou, J. Dong, Y. Luo, Q. Zhao, T. Xie, Dynamic covalent polymer networks: from old chemistry to modern day innovations, Adv. Mater. 29 (2017) 1606100.
[11] J.C. Dyre, The glass transition and elastic models of glass forming liquids, Rev. Mod. Phys. 78 (2006) 953.
[12] C.A. Angell, Formation of glasses from liquids and biopolymers, Science 267 (1995) 1924–1935.
[13] M.D. Ediger, C.A. Angell, S.R. Nagel, Supercooled liquids and glasses, J. Phys. Chem. 100 (1996) 13200–13212.
[14] M. Guerre, C. Taplan, J.M. Winne, F.E. DuPrez, Vitrimers: directing chemical reactivity to control material properties, Chem. Sci. 11 (2020) 4855–4870.
[15] F.I. Altuna, C.E. Hoppe, R.J.J. Williams, Shape memory epoxy vitrimers based on DGEBA crosslinked with dicarboxylic acids and their blends with citric acid, RSC Adv. 6 (2016) 88647–88655.
[16] T. Liu, C. Hao, L. Wang, Y. Li, W. Liu, J. Xin, J. Zhang, Eugenol-derived biobased epoxy: Shape memory, repairing and recyclability, Macromolecules 50 (2017) 8588–8597.
[17] S. Zhang, T. Liu, C. Hao, L. Wang, J. Han, H. Liu, J. Zhang, Preparation of a lignin-based vitrimer material and its potential use for recoverable adhesives, Green Chem. 20 (2018) 2995–3000.
[18] Z. Yang, Q. Wang, T. Wang, Dual-triggered and thermally reconfigurable shape memory graphene-vitrimer composites, ACS Appl. Mater. Interfaces 8 (2016) 21691–21699.
[19] A. Li, J. Fan, G. Li, Recyclable thermoset shape memory polymers with high stress and energy output: via facile UV-curing, J. Mater. Chem. A 6 (2018) 11479–11487.
[20] T.F. Scott, A.D. Schneider, W.D. Cook, C.N. Bowman, Photoinduced plasticity in cross-linked polyners, Science 308 (2005) 1615–1617.
[21] A. Rekondo, R. Martin, A. Ruiz de Luzuriaga, Germán Cabañero, Hans J. Grande, I. Odriozola, Catalyst-free room temperatura self-healing elastomers base on aromatic disulfide metathesis, Mater. Horiz. 1 (2014) 237–240.
[22] (a) A. Ruiz de Luzuriaga, R. Martin, N. Markaide, A. Rekondo, G. Cabañero, J. Rodríguez, I. Odriozola, Mater. Horizons 3 (2016) 241–247. (b) A. Ruiz de Luzuriaga, R. Martin, N. Markaide, A. Rekondo, G. Cabañero, J. Rodríguez, I. Odriozola, Mater. Horizons. https://doi.org/10.1039/D0MH90047H.
[23] Z. Ma, Y. Wang, J. Zhu, J. Yu, Z. Hu, Bio-based epoxy vitrimers: reprocessibility, controllable shape memory, and degradability, J. Polym. Sci., Part A: Polym. Chem. 55 (2017) 1790–1799.
[24] F. Ji, X. Liu, D. Sheng, Y. Yang, Epoxy-vitrimer composites based on exchangeable aromatic disulfide bonds: reprocessibility, adhesive, multi-shape memory effect, Polymer 197 (2020) 122514.
[25] H. Memon, Y. Wei, Welding and reprocessing of disulfide-containing thermoset epoxy resin exhibiting behavior reminiscent of a thermoplastic, J. Appl. Polym. Sci. (2020) e49541.
[26] A. Genua, S. Montes, I. Azcune, A. Rekondo, S. Malburet, B. Daydé-Cazals, A. Graillot, Build-to-specification vanillin and phloroglucinol derived biobased epoxy-amine vitrimers, Polymers 12 (2020) 2645.
[27] C. Di Mauro, S. Malburet, A. Graillot, A. Mija, Recyclable, repairable, and reshapable (3R) thermoset materials with shape memory properties from bio-based epoxidized vegetable oils, ACS Appl. Bio. Mater. 3 (2020) 8094–8104.
[28] H. Si, L. Zhou, Y. Wu, L. Song, M. Kang, X. Zhao, M. Chen, Rapidly reprocessable, degradable epoxy vitrimer and recyclable carbon fiber reinforced thermoset composites relied on high contents of exchangeable aromatic disulfide crosslinks, Compos. Part B: Eng. 199 (2020) 108278.
[29] Y. Spiesschaert, C. Taplan, L. Stricker, M. Guerre, J.M. Winne, F.E. Du Prez, Influence of the vitrimer matrix on the viscoelastic behavior of vitrimers, Polym. Chem. 11 (2020) 5377–5385.
[30] T. Xie, I.A. Rousseau, Facile tailoring of thermal transition temperatures of epoxy shape memory polymers, Polymer 50 (2009) 1852–1856.
[31] F.W.A. Su, K.C. Chen, S.Y. Tseng, Effects of chemical structure changes on thermal, mechanical, and crystalline properties of rigid rod epoxy resins, J. Appl. Polym. Sci. 78 (2000) 446–451.
[32] J.M. Matxain, J.M. Asua, F. Ruiperez, Design of new disulfide-based organic compounds for the improvement of self-healing materials, PCCP 18 (2016) 1758–1770.
[33] S. Nevejans, N. Ballard, J.I. Miranda, B. Reck, J.M. Asua, The underlying mechanism for self healing of poly(disulfide)s, PCCP 18 (2016) 27577–27583.